

Simulation and experiment of the cooling effect of trapped ion by pulsed laser

Chang-Da-Ren Fang(方长达人), Yao Huang(黄垚), Hua Guan(管桦), Yuan Qian(钱源), and Ke-Lin Gao(高克林)
Citation: Chin. Phys. B, 2021, 30 (**7**): 073701. DOI: 10.1088/1674-1056/abf91f
Journal homepage: http://cpb.iphy.ac.cn; http://iopscience.iop.org/cpb

What follows is a list of articles you may be interested in

Direct loading of atoms from a macroscopic quadrupole magnetic trap into a microchip trap

Jun Cheng(程俊), Jing-fang Zhang(张敬芳), Xin-ping Xu(许忻平), Hai-chao Zhang(张海潮), Yu-zhu Wang(王育竹)
Chin. Phys. B, 2017, 26 (**3**): 033701. DOI: 10.1088/1674-1056/26/3/033701

Theoretical derivation and simulation of a versatileelectrostatic trap for cold polar molecules

Shengqiang Li(李胜强)
Chin. Phys. B, 2016, 25 (**11**): 113702. DOI: 10.1088/1674-1056/25/11/113702

Determination of ion quantity by using low-temperature ion density theory and molecular dynamics simulation

Du Li-Jun, Song Hong-Fang, Li Hai-Xia, Chen Shao-Long, Chen Ting, Sun Huan-Yao, Huang Yao, Tong Xin, Guan Hua, Gao Ke-Lin
Chin. Phys. B, 2015, 24 (**11**): 113703. DOI: 10.1088/1674-1056/24/11/113703

Fast thermometry for trapped atoms using recoil-induced resonance

Zhao Yan-Ting, Su Dian-Qiang, Ji Zhong-Hua, Zhang Hong-Shan, Xiao Lian-Tuan, Jia Suo-Tang
Chin. Phys. B, 2015, 24 (**9**): 093701. DOI: 10.1088/1674-1056/24/9/093701

Structured mirror array for two-dimensional collimation of a chromium beam in atom lithography

Zhang Wan-Jing, Ma Yan, Li Tong-Bao, Zhang Ping-Ping, Deng Xiao, Chen Sheng, Xiao Sheng-Wei
Chin. Phys. B, 2013, 22 (**2**): 023701. DOI: 10.1088/1674-1056/22/2/023701

Simulation and experiment of the cooling effect of trapped ion by pulsed laser*

Chang-Da-Ren Fang(方长达人)[1,2,3], Yao Huang(黄垚)[1,2], Hua Guan(管桦)[1,2], Yuan Qian(钱源)[1,2,3], and Ke-Lin Gao(高克林)[1,2,†]

[1] State Key Laboratory of Magnetic Resonance and Atomic and Molecular Physics, Innovation Academy for Precision Measurement Science and Technology, Chinese Academy of Sciences, Wuhan 430071, China
[2] Key Laboratory of Atomic Frequency Standards, Innovation Academy for Precision Measurement Science and Technology, Chinese Academy of Sciences, Wuhan 430071, China
[3] School of Physical Sciences, University of Chinese Academy of Sciences, Beijing 100049, China

(Received 8 March 2021; revised manuscript received 13 April 2021; accepted manuscript online 19 April 2021)

We investigate the process of pulsed laser cooling using a self-constructed molecular dynamics simulation (MD-Simulation) program. We simulate the Doppler cooling process and pulsed laser Doppler cooling process of a single $^{40}Ca^{+}$ ion, and the comparison with the experimental results shows that this self-constructed MD-Simulation program works well in the weak laser intensity situation. Furthermore, we analyze the pulsed laser Doppler cooling process of a single $^{27}Al^{+}$ ion. This program can be used to analyze the molecular dynamic process of various situations of Doppler cooling in an ion trap, which could give predictions and experimental guidance.

Keywords: doppler cooling, pulsed laser cooling, molecular dynamics simulation

PACS: 37.10.Vz, 87.10.Tf **DOI:** 10.1088/1674-1056/abf91f

1. Introduction

In the past two decades, optical clock technology has been developed rapidly and has currently become the frequency standard with the best accuracy and stability, and it has many potential applications in timing, precision measurement physics, verification of fundamental physical theories, detection of dark matter and gravitational waves, etc.[1–9] At the same time, new candidate systems for optical clocks have been proposed, such as highly charged-ion-based (HCI) optical clocks, and nuclear-based optical clocks.[10–12] The reference transitions for these above-mentioned clocks are insensitive to the external field, thus these clocks are considered to be one of the next-generation optical clocks with higher precision. However, for the above-mentioned clock candidates, the wavelengths of the cooling lasers are often in the deep ultraviolet (DUV) range. Though with the development of DUV laser technology, lasers with wavelengths in the order of tens of nanometers have been made,[13–16] no CW laser with wavelength less than 170 nm has been reported yet. At present, for a reference system with a cooling laser wavelength less than 170 nm, such as $^{27}Al^{+}$ ion optical clock[17] and HCI optical clock,[10,11] sympathetic cooling method is required, and the state readout for the optical clock is realized indirectly with the quantum logic measurement scheme,[18] which requires complicate cooling processes such as sideband cooling, which could increase the technical complexity of optical clock implementation, meanwhile, additional uncertainty would be brought in by this scheme due to the existence of sympathetic-cooling ions.[19] If DUV pulsed laser can be used for cooling these ions directly, the uncertainties of these optical clocks will be expected to be even smaller.

The following key parameters that should be considered when studying whether DUV pulsed laser can be used to cool ions are: the pulse width, duty ratio, and the linewidth of the pulsed laser, the heating rate of the ion trap, etc. Taking the $^{27}Al^{+}$ clock as an example, the required cooling laser wavelength is 167 nm; while a 167 nm DUV pulsed laser had been made by Technical Institute of Physics and Chemistry, CAS, thanks to the development of deep-ultraviolet diode laser-pumped solid-state lasers (DUV-DPL). The pulse width is 200 μs with a duty ratio of only 1‰ limited by technical reasons related to the crystal growth.[20,21] It can be expected that the pulsed laser Doppler cooling effect for ions with low duty cycle should be different from that by continuous laser, which makes the efficiency and effectiveness of pulsed laser cooling has become a valuable research topic.

Many research groups in the world have conducted related research on pulsed laser cooling. In 1991, Mølmer proposed to utilize pulsed lasers with pulse width similar to the lifetime of upper state of the cooling cycle to cool atoms, which may lead to a temperature limitation below the Doppler

*Project supported by the National Key Research and Development Program of China (Grant No. 2017YFA0304401), the National Development Project for Major Scientific Research Facility, China (Grant No. ZDYZ2012-2), the National Natural Science Foundation of China (Grant Nos. 11774388 and 11634013), the Strategic Priority Research Program of the Chinese Academy of Sciences (Grant No. XDB21030100), the CAS Youth Innovation Promotion Association (Grant Nos. 2018364 and Y201963), and the K. C. Wong Education Foundation (Grant No. GJTD-2019-15).

†Corresponding author. E-mail: klgao@apm.ac.cn

© 2021 Chinese Physical Society and IOP Publishing Ltd

cooling limit.[22] In 2006, Monroe's group from the University of Michigan used ultrafast pulsed lasers for cooling the Cd^+ ion, reaching a temperature of 1 K.[23] In 2014, the National Institute of Information and Communications Technology of Japan successfully excited the $^1S_0$–$^1P_1$ state transition of In^+ at 159 nm with vacuum DUV laser generated by high-order harmonics in the cavity, since the power is only 6.5 μW, this laser can only be used for detection but cannot achieve laser cooling.[24] In 2016, Udem *et al.* at Max-Planck Institute tried to use ultraviolet comb for Doppler cooling of Mg ion,[25] while the sympathetic cooling method is still needed in the cooling process due to the heating effect caused by the blue detuned "comb teeth". In a word, pulse laser has not been used for mK level ion laser cooling in the world. What is the efficiency and effectiveness of pulse laser cooling? It is still an urgent problem to be solved.

In this paper, we have studied the efficiency and effectiveness of pulsed laser cooling in combination of simulation and experiment. First of all, in the experiment, we take the $^{40}Ca^+$ ion as a research object, using the acousto-optic modulator (AOM) to modulate a continuous 397 nm laser for generating a parameter adjustable pulse laser. By adjusting the detuning and power, we optimize the effect of the Doppler cooling, and then measure the cooling result. In addition, we propose an optimized molecular dynamics (MD) simulation program to simulate the Doppler cooling process of in the ion trap. The simulations include the background heating process, continuous laser Doppler cooling process and pulsed laser Doppler cooling process. The results of comparison between the computer simulations and the experiments show that this MD-Simulation program is effective in weak laser intensity situation. Next, we use this MD-simulation method to analyze the possibility of pulsed laser cooling of $^{27}Al^+$ as an example. This method can also be extended to other systems such as HCI optical clocks and nuclear optical clocks.

2. Optimized molecular dynamics simulation

The laser cooling process of the trapped ion is primarily affected by: (1) radio frequency (RF) field and axial electrostatic potential trapping force; (2) Coulomb interaction among ions; (3) laser cooling force; (4) random interaction forces between ions and the environment in an ion trap such as residual background gas in the vacuum chamber. The kinetic equation of a specific ion in the system can be expressed as[26]

$$\begin{aligned} M_i \frac{\mathrm{d}\boldsymbol{r}_i^2}{\mathrm{d}^2 t} &= \boldsymbol{F}_i(\boldsymbol{r}_1,\ldots,\boldsymbol{r}_N,\boldsymbol{v}_1,\ldots,\boldsymbol{v}_N,t) \\ &= \boldsymbol{F}_i^{\mathrm{trap}} + \boldsymbol{F}_i^{\mathrm{Coulomb}} + \boldsymbol{F}_i^{\mathrm{laser}} + \boldsymbol{F}_i^{\mathrm{random}}, \end{aligned} \tag{1}$$

where $i = 1,\ldots,N$ denote every specific ion in a system with N ions. M_i, $\boldsymbol{r}_i$, $\boldsymbol{v}_i$ denote the mass, position vector and velocity vector of the i-th ion, respectively.[27]

The electric potential field force applied on the i-th ion can be obtained as follows:

$$\boldsymbol{F}_i^{\mathrm{trap}} = q_i \nabla \varphi\,(x,y,z,t)\,, \tag{2}$$

where q_i is the charge of the i-th ion, and the expression of the trapped potential field is

$$\begin{aligned} \varphi\,(x,y,z,t) \;=\; & \frac{\alpha U_{\mathrm{RF}}}{2}\left(1+\frac{x^2-y^2}{r_0^2}\right)\cos\left(\Omega_{\mathrm{RF}}t\right) \\ & + \frac{\kappa U_{\mathrm{ec}}}{L^2}\left(z^2-\frac{x^2+y^2}{2}\right), \end{aligned} \tag{3}$$

where α and κ are the radial and axial geometry factors, respectively, which are introduced because the electrodes are not perfect parabola and will be shielded by other electrodes. U_{RF} is the RF field voltage amplitude, Ω_{RF} is the RF field angular frequency, U_{ec} is the cap voltage, r_0 is the distance between the tip of the blade and the axis of the trap, and L is the tip distance between the two caps.

The Coulomb interaction force experienced by the i-th ion can be obtained by superimposing the Coulomb force exerting on the i-th ion by all other ions, which can be expressed as

$$\boldsymbol{F}_i^{\mathrm{Coulomb}} = \frac{q_i}{4\pi\varepsilon_0}\nabla\left[\sum_{j\neq i}\frac{q_j}{r_{ji}}\right] = \sum_{j\neq i}\frac{q_i q_j \boldsymbol{r}_{ji}}{4\pi\varepsilon_0 r_{ji}^3}, \tag{4}$$

where $\boldsymbol{r}_{ji}$ is the position vector of the i-th ion relative to the j-th ion, and ε_0 is the vacuum permittivity.

The force applied on the ion induced by the laser field can be expressed as[28]

$$\boldsymbol{F}^{\mathrm{laser}} = \frac{\hbar\boldsymbol{k}\Gamma}{2}\frac{s}{1+s+4(\delta-\boldsymbol{k}\cdot\boldsymbol{v})^2/\Gamma^2}, \tag{5}$$

where $\boldsymbol{v}$ is the velocity vector of the ion, Γ is the natural line width, δ is the detuning of the laser, and $\boldsymbol{k}$ is the wave vector of the laser. The parameter $s = \left(\Omega_{\mathrm{Rabi}}^2/2\right)/\left(\Delta\omega^2+\Gamma^2/4\right)$ is the saturation parameter, in which Ω_{Rabi} is the Rabi frequency, $s_0 = 2\Omega_{\mathrm{Rabi}}^2/\Gamma^2 = I/I_{\mathrm{sat}}$ when $\Delta\omega = 0$, in which $I_{\mathrm{sat}} = 2\pi^2\hbar c\Gamma/3\lambda_{\mathrm{Laser}}^3$ is the saturation laser power intensity.[28]

The laser force of low temperature ions can be approximated with low order expression around $v = 0$: $\boldsymbol{F} = \boldsymbol{F}_0 - \beta\cdot\boldsymbol{v} + o\left(\boldsymbol{v}^2\right)$, where $\boldsymbol{F}_0 = (\hbar\boldsymbol{k}s/2)/[1+s+4\left(\delta/\Gamma\right)^2]$ can be interpreted as the average radiation pressure applied on the ion, while the effect of $\boldsymbol{F}^{\mathrm{cooling}} = -\beta\cdot\boldsymbol{v}$ depends on the coefficient $\beta = -4\hbar\boldsymbol{k}^2 s\delta/[\Gamma\cdot(1+s+4\delta^2/\Gamma^2)^2]$. When the laser is red detuned, which means the detuning $\delta < 0$, the $\boldsymbol{F}^{\mathrm{cooling}} = -\beta\cdot\boldsymbol{v}$ is opposite to the ion's velocity all the time like a damping force, which decelerates the ion. On the contrary, when the detuning $\delta > 0$, the damping coefficient $\beta < 0$, which leads to a heating force.

When the ion temperature is high, the high-order effect of the laser on ion cannot be ignored, so we take the original expression (5) into the simulation. On the other hand, we use the formula $\boldsymbol{F}^{\mathrm{L-random}} = \boldsymbol{r}_{\mathrm{random}}\cdot$

$(\hbar k\Gamma s)/2(1+s+4(\delta-\boldsymbol{k}\cdot\boldsymbol{v})^2/\Gamma^2)$ to express the force induced by the spontaneous emission, which was often ignored in previous MD-simulation programs, where $\boldsymbol{r}_{\text{random}}$ denotes a random direction of the spontaneous emission.

Due to the non-ideal characteristics of the experimental environment such as the effect of the background gas, the limited machine precision of the trap, the electric noise on the RF voltage, we can ignore the effect of random background heating. We assume that the random background heating force $\boldsymbol{F}^{\text{random}}$ is isotropic, which obeys a normal distribution $N(0, 2mP/\Delta t)$, where m is the ion mass, P is the heating rate of the trap measured in the experiment. The motion of the ion under the action of this random force behaves as Brownian random walk stochastic process in its momentum space, which leads to a heating effect. Using the relevant conclusions of Brownian motion and the relation between the chi-square distribution and the normal distribution, we can obtain

$$\begin{aligned}\langle E_k(t)\rangle &= \left\langle \frac{1}{2}m\boldsymbol{v}^2 \right\rangle = E_k(0)+\overline{P}\cdot t;\\ \mathrm{SD}[E_k(t)] &= \mathrm{SD}\left[\frac{1}{2}m\boldsymbol{v}^2\right] = \sqrt{2}\overline{P}\cdot t,\end{aligned} \tag{6}$$

where $\langle\cdots\rangle$ indicates carrying out the expectation value of the variables in brackets, $\mathrm{SD}[\cdots]$ represents the standard deviation of the variables in the brackets. Formulas (6) imply that the mean (expected) value and standard deviation of the total kinetic energy of the particle increase linearly with time, under the action of the assumed force $\boldsymbol{F}^{\text{random}}$.

Finally, we introduce time-dependent laser force to simulate the action process of pulsed laser on ions and use leap-frog algorithm[29–31] to simulate the dynamic process of the ions.

3. Experiment for the Doppler cooling of $^{40}Ca^+$ with pulsed laser

We chose $^{40}Ca^+$ ion as the research object in the experiment. Due to the lack of pulse laser, we used an acousto-optic modulator to switch continuous laser to produce pulsed laser, using time sequence we could control and adjust the pulse width and duty ratio of the pulsed laser. A slightly modified new type of trap, which was first designed by NIST,[32] was used in this experiment. This ion trap has a low heating rate, which is conducive to long-term stable ion trapping, and the cooling effect may also reach a lower level.

The evaluation of ion temperature can be realized by observing the Rabi oscillation spectrum of the clock transition. The Rabi oscillation of the transition is weakly modulated by the ion temperature (phonon number) in the following form:[33]

$$\rho_{\text{DD}}(t) = \frac{1}{2}\left\{1-\sum_n \rho_{n,n}\cos\left[\Omega\left(1-\eta^2 n\right)t\right]\right\}. \tag{7}$$

As in the case of $^{40}Ca^+$, t is the action time of the 729 nm laser and ρ_{DD} is the population of state $3^2D_{5/2}$, the sum here iterates over all the positive integers, i.e., the phonon number is $1\sim\infty$, while $\rho_{n,n}$ indicates the population when phonon number is n. Finally, the average phonon number can be obtained by carrying out the statistical average of phonon number n, where η is the Lamb–Dicke parameter. Since the Lamb–Dicke parameter is less than 0.1 at most of the time, it is reasonable to expand the expression of Rabi frequency to first order in η^2, which leads to an approximate analytical formula:[33]

$$\rho_{\text{DD}}(t) = \frac{1}{2}\left(1-\frac{1}{\bar{n}+1}\frac{\cos(2\Omega_0 t)\left(1-x\cos\left(2\Omega_0 t\eta^2\right)\right)+x\sin(2\Omega_0 t)\sin\left(2\Omega_0 t\eta^2\right)}{1+x^2-2x\cos\left(2\Omega_0 t\eta^2\right)}\right), \tag{8}$$

where n is the average phonon number, and $x=\bar{n}/(\bar{n}+1)$.

By fitting the curve data obtained in the experiment using formula (8), average phonon number n can be obtained, while the temperature of the ion and $\bar{n}$ can be expressed as

$$T = \left(\bar{n}+\frac{1}{2}\right)\frac{\hbar\omega}{k_{\text{B}}}, \tag{9}$$

where ω is the secular motion frequency of interest, and k_{B} is the Boltzmann constant.

3.1. Heating rate measurement

The experiment can be divided into three main parts, and the sequence is shown in Fig. 1:

In the first part, we adopt a fixed near red detuned frequency for the 397 nm laser to cool the $^{40}Ca^+$ for 2000 μs. The purpose is to make each experiment starts at the identical low initial temperature (close to the Doppler cooling limit). In the second part, we turn off all the lasers and let the $^{40}Ca^+$ be heated for a while. This allows the temperature of the $^{40}Ca^+$ to rise for the measurement in the third stage. In the third part, we use a 729 nm clock transition laser for probing the $^{40}Ca^+$. After that, a 397 nm laser is used to observe the fluorescence signal of the ion, for counting the population between the states of $4^2D_{1/2}$ and $3^2D_{5/2}$, we take 75 measurements at each experimental point to get the average result. By obtaining the relation between the population and the action time of 729 nm laser, we constructed a Rabi oscillation curve to be fitted to get the temperature at each time. Finally, we got the relation between the temperature and the waiting time, i.e., the heating time, which indicates the heating rate of the trap.

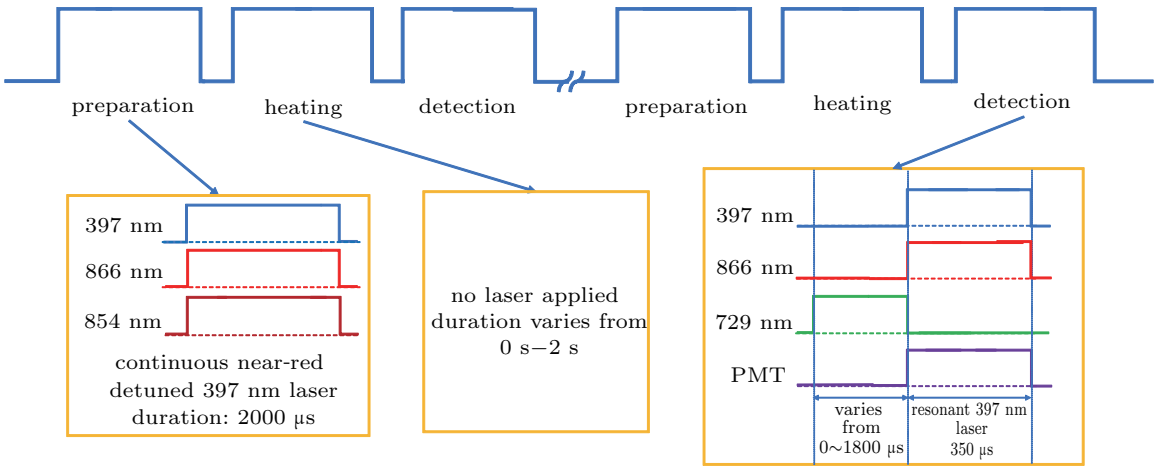


Fig. 1. Schematic for the pulse sequence in the heating rate measurement.

3.2. Doppler cooling of the $^{40}Ca^{+}$ with pulsed laser

We measured the influence of two important parameters in the experiment, which are the laser's effective pulse width and the duty ratio of the pulsed laser. The experiment can be divided into three main parts, and the sequence is shown in Fig. 2.

In the first part, we used a fixed-frequency red detuning laser to cool the $^{40}Ca^{+}$. The purpose is to make the $^{40}Ca^{+}$ at the same initial temperature at the beginning of each experiment, so that we can ensure that each experiment is carried out under the same initial conditions. The reason for using far-red detuned laser is to keep the $^{40}Ca^{+}$ at a high initial temperature for the next cooling process experiment. In the second part, we used a 397 nm pulsed laser for cooling; the pulse width, pulse number, and the duty ratio parameters of the laser were continually changed during the experiment. In the final stage, the same as the previous experiment, by detecting and fitting the Rabi oscillation diagram we obtained the ion temperature. Based on this, we can give the diagram that the temperature of $^{40}Ca^{+}$ ion changes with time under the action of 397 nm pulsed laser with given intensity, given red-detuning and given pulse on/off time parameters.

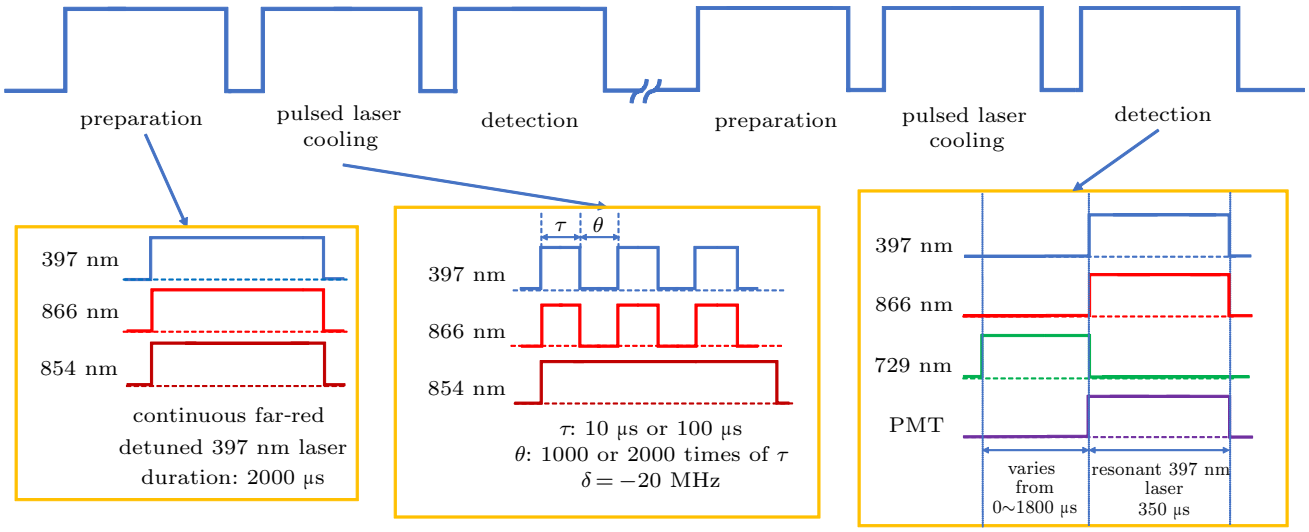


Fig. 2. Schematic for the ion temperature measurement after the laser cooling.

4. Analysis

By substituting the relevant parameters in the MD-simulation program with the measured heating rates, the pulse width and duty ratio used in the experiment, we performed the simulation. After obtaining the data derived from the MD-simulation, we put the experimental and simulation results in the same graph for comparison and analysis, as shown in Figs. 3 and 4.

It can be seen that MD-Simulation program gives a fairly consistent result in each case, some deviation of the blue dots from the simulation results could be due to the change of the experimental environment during the long period of the measuring procedure. In addition, due to the low heating rate of the ion trap used in the experiment, the on/off time of the pulsed laser does not seem to significantly affect the cooling process

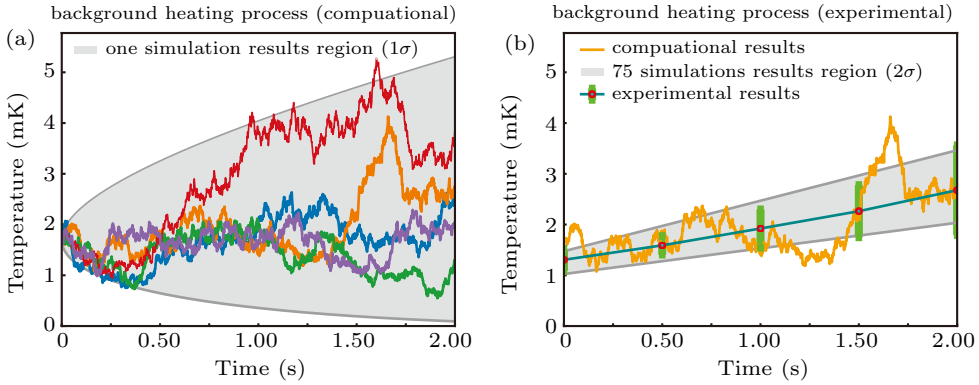


Fig. 3. (a) The heating process calculated by MD-Simulation. Each color line is one specific simulation result, since all the processes are stochastic, actually there are countless possible results, we present 5 results here in the figure without loss of generality, in the same situation of Figs. 4 and 5. The gray area indicates one standard deviation range of the single simulation result. The blue line with green bar in (b) shows the experimental results (each measurement point is an average of 75 measurements), the orange line shows one simulation result, and the gray area shows two standard deviation ranges of the average of 75 simulations.

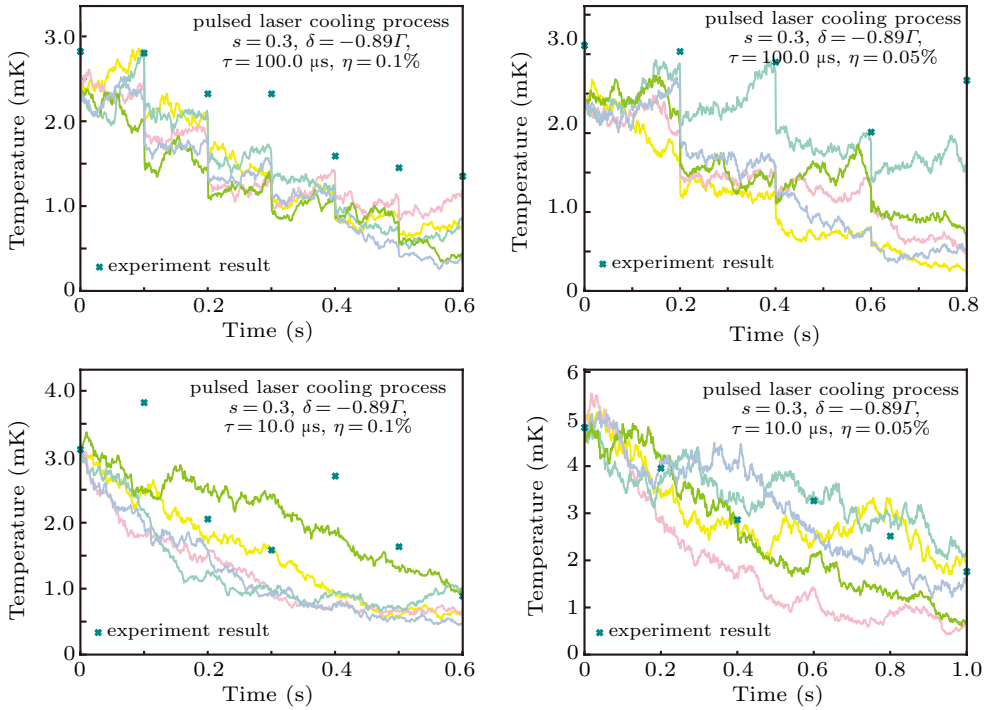


Fig. 4. Comparison between experiment and simulation of the Doppler cooling by pulsed laser. The results under different laser parameters are shown, in which the blue points represent the measured data, and the color curves represent the simulation results of several numerical calculations. Since the process is stochastic, there could be countless possible real processes, five possible results are shown in each picture.

of $^{40}Ca^{+}$. Of course, the higher the duty ratio is, the more stable the temperature variation of the ion is, while the lower the duty ratio is, the more likely the energy of the ion will change randomly during the light-off period, and the greater the temperature variance there will be. Therefore, we can observe that when the duty cycle is 1/2000, the jitter of ion's temperature appears to be larger than the situation when the duty cycle is 1/1000. It needs to be mentioned that due to the fact that the Doppler cooling process of $^{40}Ca^{+}$ (down to the Doppler cooling limit) only requires a few hundreds of microseconds under the initial conditions we have given, the laser action time of 100 μs is enough for significantly reducing the ion's temperature, and the horizontal axis in the figure is in the scale of seconds, which makes the deceleration process of 100 μs appear to be very steep in the figure.

Based on the above results, we believe this MD-Simulation program can be reasonably applied to a wider range of situations. For example, under the condition that given the duty ratio of the pulsed laser, how much should the heating rate of the trap must be controlled so that the ion can be effectively cooled? Because it is difficult to adjust the heating rate in a large range, to explore the problem by means of MD-Simulation is an effective solution.

Next, we take the $^{27}Al^{+}$ as an example, using the pulse width and duty ratio of the laser mentioned in Refs. [20,21] (the pulse width of the 167 nm pulsed laser is 200 μs, and the duty ratio is 1‰) as the input value of the model, through calculation and simulation, the possibility of using this pulsed

laser to achieve Doppler laser cooling of the $^{27}Al^+$ has been explored.

Through a simple analysis of formula (6), we can see that the interaction between laser and ion is positively correlated with Γ. When the natural width Γ is large and the detuning amount δ is small, the interaction $\boldsymbol{F}$ between laser and ion is almost proportional to Γ. Meanwhile, Γ_{Al^+} is about 10 times that of Γ_{Ca^+}, which means that the interaction intensity between 167 nm laser and $^{27}Al^+$ is almost 10 times that of 397 nm laser and $^{40}Ca^+$. It can be foreseeable that aluminum ions will be cooled down faster under the action of 167 nm laser, and molecular dynamics simulation does give this result. We give the temperature change of $^{27}Al^+$ in one second under the action of 167 nm pulse laser under three different trap heating rates (the initial temperature given in this direction is about 37 mK), as shown in Fig. 5.

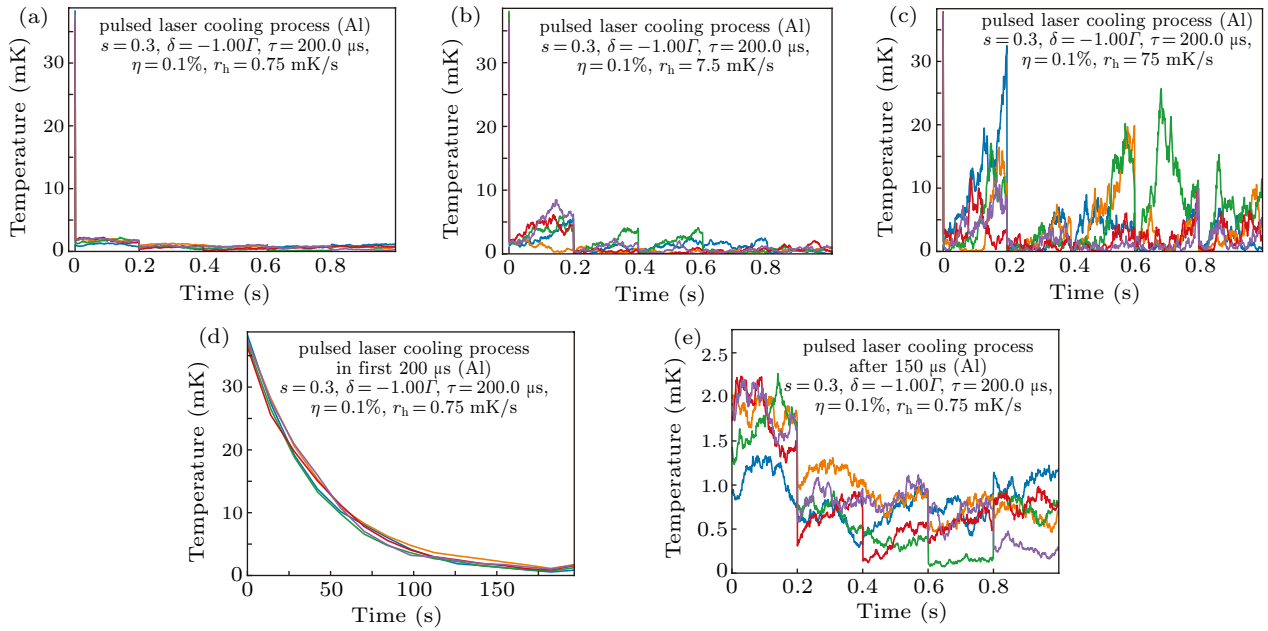


Fig. 5. Simulation results of $^{27}Al^+$ cooling by 167 nm pulse laser with pulse width of 200 μs and duty ratio of 1%. Note that the deceleration effect of the 167 nm laser on $^{27}Al^+$ is so strong that the $^{27}Al^+$ in each group of the simulations experienced the initial rapid cooling process, which leads to the sharp drop at the beginning of the curve, as shown in (a)–(c). (d) The energy change in the first 200 μs. (e) The evolution after the first 150 μs of (a), performed under these parameters: $s=0.3$, $\delta=-1.0\Gamma_{Al^+}$, $\tau=200$ μs, $\eta=0.1\%$ and $r_{heating}=0.75$ mK/s (the same phenomenon happens in (b) and (c), in which the heating rate of the trap are set to be 10 and 100 times of the original heating rate respectively with the other parameters unchanged).

We can easily derive from formula $\boldsymbol{F}=\boldsymbol{F}_0-\beta\cdot\boldsymbol{v}+o\left(\boldsymbol{v}^2\right)$ that the "cooling rate" applied by the laser is $P^{\text{cooling}}=-\beta\left\langle\boldsymbol{v}^2\right\rangle$ by taking $\langle\boldsymbol{v}\rangle=0$ into consideration and omitting the high order parts. Since Γ_{Al^+} is about 10 times of Γ_{Ca^+}, only the temperature of the ten-fold relationship between $^{27}Al^+$ and $^{40}Ca^+$ is comparable. We can see from Figs. 6(a) and 6(b) that it takes about 100 μs for the temperature of $^{40}Ca^+$ to drop from 3.2 mK to 2.38 mK, while the time for the temperature of $^{27}Al^+$ to drop from 32 mK to 23.8 mK is about 14.5 μs, in other words, the cooling rate in the situation of $^{27}Al^+$ is about 6.9 times of $^{40}Ca^+$ in the comparable temperature interval (actually, the ratio ranges between 6.6 and 7.1 considering the precision), which is consistent with Fig. 6(d). We should notice that the "cooling rate" shown in Fig. 6(c) is not the "real cooling rate" in the trap, since there are photon-recoil induced heating and background heating should be taken into consideration at least, which leads to the real cooling rate shown in Figs. 6(a) and 6(b) in one order of magnitude smaller than that shown in Fig. 6(c). In spite of that, the consistency between Fig. 6(d) and the real cooling rate ratio derived from Figs. 6(a) and 6(b) is due to the fact that the ratio of the photon-recoil heating effect of the two ions is almost the same as the ratio between the laser cooling effect (the photon-recoil effect and the photon-absorb effect have the same form, except that the photon-absorb force is directional, and the photon-recoil effect is isotropic), and the heating rate of the ion trap used in the experiment is extremely low, which does not affect the result much.

From the foregoing discussion, we can see that this MD-Simulation program gives a relatively consistent result with the experiment for the situation of $^{40}Ca^+$. On the other hand, because the laser cooling process of $^{40}Ca^+$ and $^{27}Al^+$ obey the same physical mechanism, the MD-Simulations of these two ions also give fairly consistent results as expected. In this sense, the simulation results given by this program for the situation of $^{27}Al^+$ should also be able to guide relevant experiments.

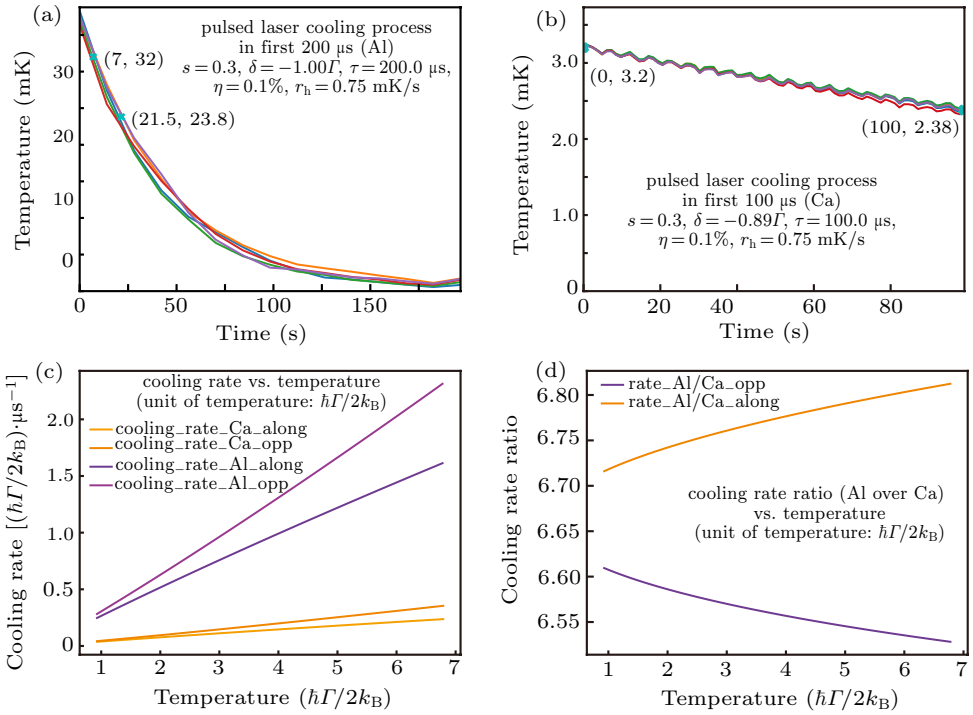


Fig. 6. Comparison between $^{27}Al^+$ and $^{40}Ca^+$. Figure 6(a) shows the first 200 μs of Fig. 5(a) while Fig. 6(b) shows the first 100 μs of Fig. 4(a). Figure 6(c) shows the cooling rate of both $^{27}Al^+$ and $^{40}Ca^+$ based on the formula $P^{\text{cooling}} = -\beta \langle v^2 \rangle$, which means how much the cooling rate the ion will experience when it is at certain average temperature (the unit of temperature has been converted to $\hbar\Gamma/2k_B$, which is the form of the Doppler cooling limit). Figure 6(d) gives the ratio of the cooling rate between $^{27}Al^+$ and $^{40}Ca^+$. The suffix _along and _opp indicate the velocity of ion is along the laser propagation direction and opposite to the laser propagation direction, respectively.

It can be seen from Fig. 5 that for ion traps with low heating rate, the pulsed laser with the parameters used above can cool $^{27}Al^+$ to the order of mK. However, as the heating rate of the trap increases, the temperature of the ions becomes difficult to control. In order to keep the temperature fluctuation above the cooling limit within 2 mK as an example, the temperature rise of $^{27}Al^+$ in the off-time, which is 200 ms, should not exceed 2 mK, which means that the heating rate of the trap should be controlled within 10 mK/s. Since the heating of the $^{27}Al^+$ mainly occurs in the off-time of the pulsed laser, as long as the temperature rises within 2 mK during this period, the 167 nm cooling laser in the next 200 μs will certainly cool it to the limit cooling temperature. When the trap heating rate reaches 100 times of the original heating rate of the trap used in our experiment, the temperature of $^{27}Al^+$ fluctuates sharply in a wide range, the $^{27}Al^+$ ion cannot be cooled effectively.

5. Conclusion

We have explored the Doppler cooling process of the ions in the ion trap by constructing a more accurate and more suitable molecular dynamics simulation program in the case of pulsed laser cooling. Compared with the experiment, the results show that the self-built MD-Simulation program does give reasonable results. In addition, we realize that the deceleration efficiency of 167 nm laser acting on $^{27}Al^+$ is about 6.6–7.1 times that of 397 nm laser acting on $^{40}Ca^+$, and that the cooling effect of 167 nm pulse laser acting on $^{27}Al^+$ is significant in 200 μs during the on-time of the pulsed laser, which means that it is not significantly different from the situation of continuous laser. Finally, the key factor to control the temperature of ions is the heating rate of the trap. As long as the heating rate is small enough, the ion temperature can be effectively reduced and controlled. According to the simulation results, the limit value of the heating rate is given. The comparison between $^{40}Ca^+$ and $^{27}Al^+$ shows that it is feasible to apply this method to the guidance of the experiment on $^{27}Al^+$.

Acknowledgment

We thank Lijun Du, Xiaozhou Yang, and Qiongli Wu for their fruitful discussions and help.

References

[1] Chou C W, Hume D B, Rosenband T and Wineland D J 2010 *Science* **329** 1630
[2] Ludlow A D, Boyd M M, Ye J, Peik E and Schmidt P O 2015 *Rev. Mod. Phys.* **87** 637
[3] Levine J 2008 *Metrologia* **45** S162
[4] Pruttivarasin T, Ramm M, Porsev S G, Tupitsyn, II, Safronova M S, Hohensee M A and Haffner H 2015 *Nature* **517** 592
[5] Lea S N 2007 *Rep. Prog. Phys.* **70** 1473
[6] Arvanitaki A, Huang J and Van Tilburg K 2015 *Phys. Rev. D* **91** 015015
[7] Derevianko A and Pospelov M 2014 *Nat. Phys.* **10** 933
[8] Stadnik Y V and Flambaum V V 2015 *Phys. Rev. Lett.* **114** 161301
[9] Reynaud S, Lamine B, Duchayne L, Wolf P and Jaekel M T 2008 *Phys. Rev. D* **77** 122003
[10] Derevianko A, Dzuba V A and Flambaum V V 2012 *Phys. Rev. Lett.* **109** 180801

[11] Kozlov M G, Safronova M S, Crespo López-Urrutia J R and Schmidt P O 2018 *Rev. Mod. Phys.* **90** 045005
[12] Peik E and Okhapkin M 2015 *Comptes Rendus Physique* **16** 516
[13] Allison T K, Cingöz A, Benko C, Yost D C, Ruehl A, Fermann M, Hartl I and Ye J 2013 *EPJ Web of Conferences* **41** 11006
[14] Benko C, Allison T K, Cingöz A, Hua L, Labaye F, Yost D C and Ye J 2014 *Nat. Photon.* **8** 530
[15] Porat G, Heyl C M, Schoun S B, Benko C, Dörre N, Corwin K L and Ye J 2018 *Nat. Photon.* **12** 387
[16] Zhang C, Schoun S B, Heyl C M, Porat G, Gaarde M B and Ye J 2020 *Phys. Rev. Lett.* **125** 093902
[17] Brewer S M, Chen J S, Hankin A M, Clements E R, Chou C W, Wineland D J, Hume D B and Leibrandt D R 2019 *Phys. Rev. Lett.* **123** 033201
[18] Schmidt P O 2005 *Science* **309** 749
[19] Zhang J, Deng K, Luo J and Lu Z H 2017 *Chin. Phys. Lett.* **34** 050601
[20] Li J J, Zhang F F, Wang Z M, Xu Y C, Guo C, Zong N, Zhang S J, Yang F, Gao H W, Yuan L, Xu F L, Liu Y, Bo Y, Cui D F, Peng Q J and Xu Z Y 2018 *IEEE J. Sel. Top. Quantum Electron.* **1600106** 6
[21] Li J J, Zhang F F, Wang Z M, Xu Y C, Liu X C, Zong N, Zhang S J, Xu F L, Yang F, Yuan L, Kou Y, Bo Y, Cui D F, Peng Q J, Wang X Y, Liu L J, Chen C T and Xu Z Y 2018 *Opt. Lett.* **43** 2563
[22] Mølmer K 1991 *Phys. Rev. Lett.* **66** 2301
[23] Blinov B B, Kohn R N, Madsen M J, Maunz P, Moehring D L and Monroe C 2006 *J. Opt. Soc. Am. B* **23** 1170
[24] Wakui K, Hayasaka K and Ido T 2014 *Appl. Phys. B* **117** 957
[25] Davila-Rodriguez J, Ozawa A, Hänsch T W and Udem T 2016 *Phys. Rev. Lett.* **116** 043002
[26] Du L J, Song H F, Li H X, Chen S L, Chen T, Sun H Y, Huang Y, Tong X, Guan H and Gao K L 2015 *Chin. Phys. B* **24** 113703
[27] Du L J, Song H F, Chen S L, Huang Y, Tong X, Guan H and Gao K L 2018 *Chin. Phys. B* **27** 043701
[28] Metcalf H J 1999 *Laser Cooling and Trapping* (New York: Springer) pp. 25, 32
[29] Verlet L 1967 *Phys. Rev.* **159** 98
[30] Verlet L 1968 *Phys. Rev.* **165** 201
[31] Zhang M Q and Skeel R D 1995 *J. Comput. Chem.* **16** 365
[32] Chen J S 2017 *Ticking near the Zero-Point Energy towards* 1×10^{-18} *Accuracy in* Al^{+} *Optical Clocks* (PhD Dessertation) (Boulder: University of Colorado) pp. 15–17
[33] Roos C 2000 *Controlling the Quantum State of Trapped Ions* (PhD Dessertation) (Innsbruck: Universiät Innsbruck) pp. 26, 117, 118